JOURNAL OF Materials CHEMISTRY

# Surface confined pseudorotaxanes with electrochemically controllable complexation properties†

**Martin R. Bryce,[a] Graeme Cooke,*[b] Florence M. A. Duclairoir,[b] Phillip John,[b] Dmitrii F. Perepichka,[a] Neil Polwart,[b] Vincent M. Rotello,[c] J. Fraser Stoddart[d] and Hsian-Rong Tseng[d]**

[a]*Department of Chemistry, University of Durham, South Road, Durham, UK DH1 3LE*
[b]*Centre for Biomimetic Design & Synthesis, Department of Chemistry, School of Engineering & Physical Sciences, Heriot-Watt University, Riccarton, Edinburgh, UK EH14 4AS. E-mail: G.Cooke@hw.ac.uk; Fax: 0131 451 3180*
[c]*Department of Chemistry, University of Massachusetts at Amherst, Amherst, MA 01002, USA*
[d]*The California Nanosystems Institute and Department of Chemistry and Biochemistry, University of California, Los Angeles, California 90095, USA*

***Received 6th June 2003, Accepted 27th June 2003***
***First published as an Advance Article on the web 24th July 2003***

A stable tetrathiafulvalene (TTF) functionalized self-assembled monolayer has been fabricated from compound **3**. The electrochemical adjustment of the guest properties of the TTF moiety of this unit has facilitated the development of surfaces in which the $\mathbf{3}^0$ state forms a pseudorotaxane with the electron deficient macrocyclic host cyclobis(paraquat-*p*-phenylene) **1**, and the electrochemically generated dicationic state $\mathbf{3}^{2+}$ forms a pseudorotaxane with the electron rich macrocyclic host 1,5-dinaphtho[38]crown-10 **2**.

## 1. Introduction

The electrochemical modulation of intermolecular interactions between host–guest complexes is a burgeoning field within supramolecular electrochemistry.[1] Electrochemically controlled supramolecular interactions between complementary host–guest moieties have been used to modulate the effectiveness of inclusion,[2] hydrogen bonded[3] and charge-transfer (C-T)[4] complexes in solution. More recently, this work has been extended to create chemically[5] and electrochemically[6] controlled redox-active host–guest complexes at the liquid/solid interface. The immobilisation of the latter systems onto conducting supports will ensure near-seamless interfacing to contemporary silicon-based input/output platforms, thereby facilitating their convenient fabrication as nanodevices.[5b,6] Moreover, the reversibility possible with electrochemically controlled host–guest interactions will allow convenient modification of surface properties and function, thereby affording a facile route to the development of responsive surfaces. For the majority of the redox controlled supramolecular systems studied to date, the switching properties have been limited to the modulation of host–guest binding between an immobilised host and a single complementary guest in solution. The development of systems whereby electrochemistry can modulate the binding between a host and multiple guest species in solution will undoubtedly find new applications within nanotechnology due to their enhanced ability to control surface structure and properties, thereby increasing their ability to handle and process information at the molecular level.[4d,7]

It has previously been shown using a combination of NMR spectroscopy and X-ray crystallography that tetrathiafulvalene in its neutral state has the propensity to form a pseudorotaxane with the electron deficient macrocycle cyclobis(paraquat-*p*-phenylene) **1**,[4d,8] whereas in its dicationic state it forms a pseudorotaxane with the electron rich cyclophane 1,5-dinaphtho[38]crown-10 **2**.[4d] Moreover, it has also been shown using cyclic voltammetry and spectroelectrochemistry[4a] that pseudorotaxane threading–dethreading can be controlled by adjusting the TTF unit's redox state. Here, we have investigated the electrochemically controllable complexation between TTF derivative **3** and macrocycles **1** and/or **2**. In particular, by exploiting the multistage redox behaviour of tetrathiafulvalene unit **3**, we have been able to take our first steps towards the fabrication of electrochemically controllable multi-pole switches in solution[4d] and at the solid/liquid interface of a monolayer (Fig. 1).[9]

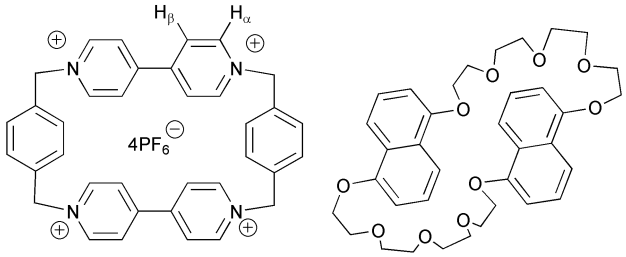


**1**



**2**

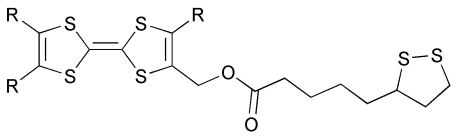

**3** R = $CH_3$
**4** R = H

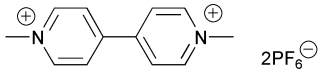


**5**

†Electronic supplementary information (ESI) available: further experimental and theoretical data. See http://www.rsc.org/suppdata/jm/b3/b306274k/

DOI: 10.1039/b306274k

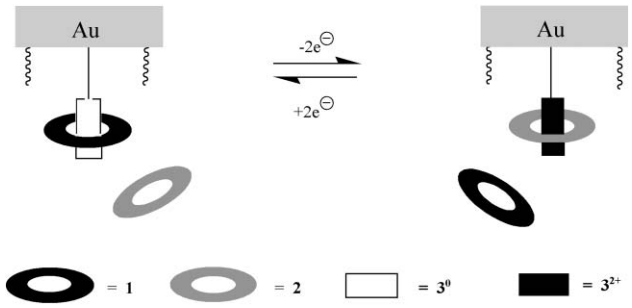


**Fig. 1** Schematic representation of electrochemically controllable surfaces that can bind with two different macrocycles in solution by adjusting the oxidation state of the immobilised host.

## 2. Results and discussion

### Molecular design and synthesis

In earlier work, we reported the fabrication of the electrochemically controlled pseudorotaxane **1·4**, whose disassembly can be controlled in solution and at the solid/liquid interface of a self-assembled monolayer (SAM).[6d] Upon electrochemical oxidation of the TTF moiety of **4**, the observed positive shift in the radical cation wave of **4** was indicative of macrocycle **1** dethreading from the TTF host unit. However, in more recent studies performed upon this system much smaller perturbations in the radical cation state of around +5 to +10 mV were often observed, compared to the +19 mV shift observed for the same process in solution. Thus, the tetraalkyl-TTF moiety was selected for this study in view of the ability of tetraalkyl-TTF derivatives to form electro-reversible complexes with **1**, with stronger binding than TTF itself.[10] Moreover, the large shifts in the radical cation oxidation wave which accompany the dethreading of pseudorotaxanes formed from tetraalkyl-TTF derivatives and **1** in solution, will significantly aid the detection of similar processes at the solid/liquid interface, where our recent studies have shown that smaller shifts occur. Macrocycles **1**[11] and **2**[12] were prepared using previously reported methods. The electroactive disulfide **3** was readily synthesised in good yield by the DCC–DMAP catalysed esterification of 4-(hydroxymethyl)-trimethylTTF[13] and thioctic acid.

### Solution complexation studies

Solution-phase complexation between **1** and **3** was confirmed by UV-vis and $^1$H NMR spectroscopic studies. Mixing **1** and **3** in equimolar proportions in MeCN resulted in an immediate formation of an emerald green-coloured solution as evidenced by the appearance of a C-T absorption band centred at $\lambda_{max}$ = 897 nm. An association constant ($K_a$) for the **1·3** complex of $4.5 \times 10^4$ $M^{-1}$ was obtained using a spectrophotometric dilution method (with MeCN as solvent).[14] The $^1$H NMR spectrum of the green-coloured complex **1·3** shows small, but significant, changes in chemical shifts relative to those of non-complexed **1** and **3**, and are consistent with the TTF unit being located "inside" the cyclophane **1** (Table 1).[8,10] FAB-MS studies of **1·3** afforded peaks at $m/z$ = 1565, 1420, 1275 which correspond to the $[M^+]$, $[M^+ - PF_6^-]$, $[M^+ - 2PF_6^-]$ ions, respectively (see ESI†).

We have modelled the C-T system **1·3** using our previously reported procedure (see ESI†).[10] The modelled structure predicts that the dimethyl-functionalized dithiole moiety is more deeply inserted within the cyclophane's cavity than the thioctic acid functionalised dithiole unit. This is consistent with the experimental data observed in solution, as $^1$H NMR spectra of **1·3** show a more pronounced shift for the 4′,5′-$CH_3$ protons of the TTF unit compared to the 4-$CH_2O$ or the 5-$CH_3$ protons.

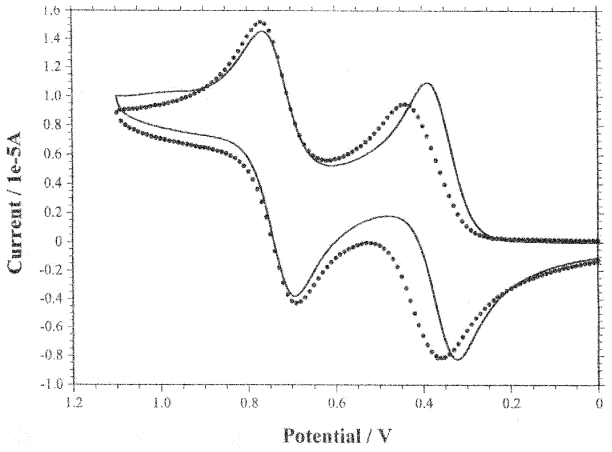


**Fig. 2** Cyclic voltammetry studies of **3** (—) and in the presence of an excess of **1** (···) [0.1 M $Bu_4NPF_6$ in $(CH_3)_2CO$].

The solution electrochemistry of **3** studied using cyclic voltammetry (CV), gave rise to two reversible oxidations at $E^1_{½}$ = +0.36 V and $E^2_{½}$ = +0.73 V (0.1 M $Bu_4NPF_6$ in $(CH_3)_2CO$) corresponding to the formation of $\mathbf{3}^{+\bullet}$ and $\mathbf{3}^{2+}$, respectively. Upon the addition of a 50-fold excess of **1** to the CV cell, the oxidation giving rise to the $\mathbf{3}^{+\bullet}$ species is immediately displaced by + 60 mV, whilst the oxidation due to the formation of $\mathbf{3}^{2+}$ is largely unaffected ($E^1_{½}$ = +0.42 V and $E^2_{½}$ = +0.73 V), suggesting that **1·3** reversibly decomplexes when the $\mathbf{3}^0$ guest experiences its first electrochemical oxidation to form the $\mathbf{3}^{+\bullet}$ state (Fig. 2).[4d] We have also investigated the electrochemically controlled complexation of **3** with compound **5** in solution. Clearly, the non-macrocyclic nature of **5** prevents inclusion of guest **3**, and as a result different electrochemical data resulting from the addition of **5** to the CV cell would be expected. Unfortunately, compound **5** has limited solubility in $(CH_3)_2CO$. However, when the CVs of compound **3** were recorded in $CH_3CN$–$CH_2Cl_2$ (80 : 20 v/v) in the presence of excess **1** (Fig. 3) or **5** (Fig. 4), significantly differing data were obtained. For the former case, a + 50 mV shift in the redox wave for the formation of the $\mathbf{3}^{+\bullet}$ state was observed, whereas the addition of species **5** to a solution of **3** resulted in a *ca.* −40 mV shift in the half-wave potentials for both the $\mathbf{3}^{+\bullet}$ and $\mathbf{3}^{2+}$ states. By comparing these data with previously reported electrochemical data for TTF upon the addition of **1**,[4d] we conclude that **3** dethreads from the cavity of cyclophane **1** upon electrochemical oxidation of the TTF component of pseudorotaxane **1·3**.

CV studies of **3** performed in $CH_2Cl_2$ containing 0.1 M $Bu_4NPF_6$, gave rise to two reversible oxidations at $E^1_{½}$ = +0.31 V and $E^2_{½}$ = +0.83 V. The addition of a 50-fold excess of **2** to the CV cell resulted in a −60 mV shift in the oxidation

**Table 1** The $^1$H NMR chemical shift data ($\delta$ and $\Delta\delta$ ) for **1**, **3** and **1·3** in $CD_3CN$ at ambient temperatures

| Compound or complex | α-Bipy-CH | β-Bipy-CH | $C_6H_4$ | 4-$CH_2O$(TTF) | 5-$CH_3$(TTF) | 4′,5′-$CH_3$(TTF) |
|---|---|---|---|---|---|---|
| **1** | 8.90 | 8.16 | 7.55 | | | |
| **3** | | | | 4.78 | 2.06 | 1.96 |
| **[1·3]** | 9.05 | 7.89 | 7.69 | 4.83 | 2.13 | 1.74 |
| $\Delta\delta$ | (+0.15) | (−0.27) | (+0.14) | (+0.05) | (+0.07) | (−0.22) |

[a]α and β are with respect to N in the cyclophane.

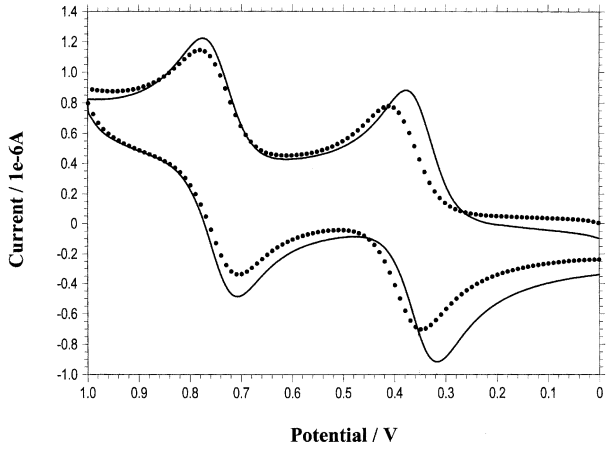


**Fig. 3** Cyclic voltammetry studies of **3** (—) and in the presence of an excess of **1** (···) [0.1 M $Bu_4NPF_6$ in $CH_3CN$–$CH_2Cl_2$ (80 : 20, v/v)].

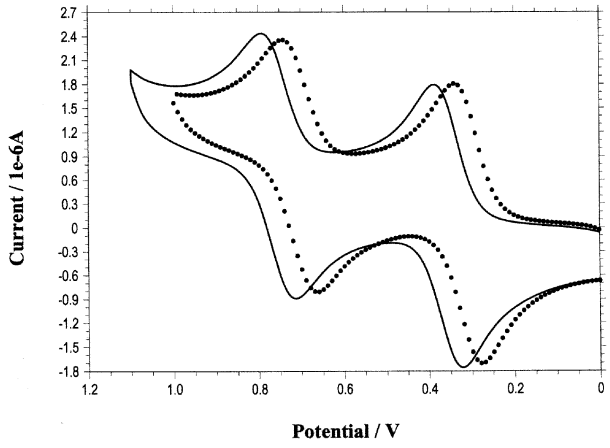


**Fig. 4** Cyclic voltammetry studies of **3** (—) and in the presence of an excess of **5** (···) [0.1 M $Bu_4NPF_6$ in $CH_3CN$–$CH_2Cl_2$ (80 : 20, v/v)].

wave for the formation of $\mathbf{3}^{2+}$, whilst the oxidation wave for the formation of $\mathbf{3}^{+\bullet}$ is largely unaffected ($E^1_{½}$ = +0.31 V and $E^2_{½}$ = +0.77 V) (Fig. 5), suggesting that $\mathbf{1}\cdot\mathbf{3}^{2+}$ undergoes a reversible decomplexation when $\mathbf{3}^{2+}$ is first reduced. When the experiments were repeated in $(CH_3)_2CO$ or $CH_3CN$ (containing 0.1 M $Bu_4NPF_6$), the addition of a 50-fold excess of **2** usually resulted in a considerably smaller shift (−20 mV) in the half-wave potential for the formation of $\mathbf{3}^{2+}$, whilst the redox wave for the formation of $\mathbf{3}^{+\bullet}$ is largely unaffected. This

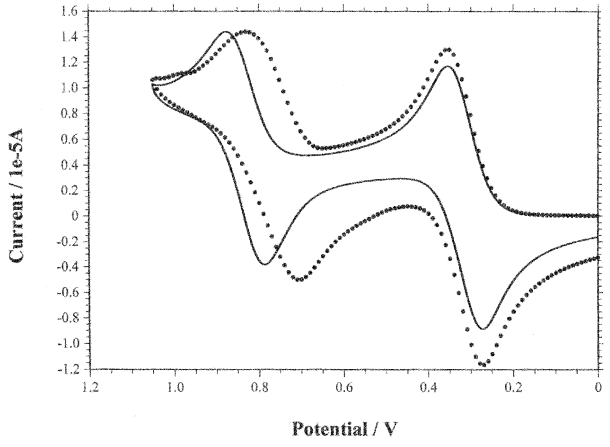


**Fig. 5** Cyclic voltammetry studies of **3** (—) and in the presence of an excess of **2** (···) [0.1 M $Bu_4NPF_6$ in $CH_2Cl_2$].

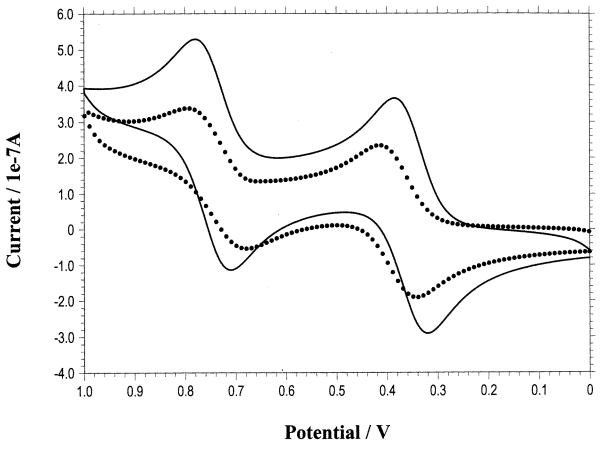


**Fig. 6** Cyclic voltammetry studies of **3** (—) and in the presence of an excess of **1** and **2** (···) [0.1 M $Bu_4NPF_6$ in $CH_3CN$–$CH_2Cl_2$ (80 : 20, v/v), scan rate = 0.01 V $s^{-1}$].

smaller shift is presumably due to a combination of the poor solubility of host **2** and better solvation of the dicationic species in $(CH_3)_2CO$ or $CH_3CN$. Finally, CV experiments were performed on **3** when both **1** and **2** were present in excess. In order to ensure reasonable solubility of both macrocycles, whilst still retaining a reversible waveform for the TTF unit in the SAM studies which were to follow, we utilised an 80 : 20 v/v mixture of $CH_3CN$ and $CH_2Cl_2$ (containing 0.1 M $Bu_4NPF_6$). The addition of **1** and **2** to the electrolyte solution caused the half-wave potential for the oxidation wave corresponding to the formation of the $\mathbf{3}^{+\bullet}$ state to be typically shifted by +30 mV, whereas the half-wave potential oxidation wave for the $\mathbf{3}^{2+}$ state was displaced by −25 mV, which is consistent with the TTF guest moiety interchanging between the two hosts upon altering its oxidation state from 0 to +2 (Fig. 6).[4d] Interestingly, the reversibility of the redox wave for the formation of the $\mathbf{3}^{2+}$ state was shown to be dependent upon scan rate; at fast scan rates (1 V $s^{-1}$) the redox wave was irreversible whereas at slower scan rates ($\leqslant$100 mV $s^{-1}$) a more reversible redox wave was obtained for this process (see ESI†). When the same experiments were repeated without the macrocycles being present, reversible redox waves were obtained for the radical cation and dication states of the TTF unit (see ESI†). We conclude that the data are consistent with a slow complexation occurring between the $\mathbf{3}^{2+}$ species and **2**, following macrocycle **1** first dethreading from the oxidised TTF unit. This presumably arises from the strong association of the components of the pseudorotaxane $\mathbf{1}\cdot\mathbf{3}$.

## Formation of self-assembled monolayers

SAMs were fabricated by immersing a gold wire (99.999%, length 70 mm, diameter 0.5 mm) in a solution of **3** (1 mmol) in MeCN for 24 hours. After washing the electrode with THF and MeCN and allowing it to dry in air, the SAM modified electrodes were placed in a solution of 0.1 M $Bu_4NPF_6$ and their CVs were recorded. The reversibility of the redox waves of immobilized **3** are critically dependent upon the solvent in which the CVs are recorded; for example, reversible oxidation waves for the electrochemical formation of $\mathbf{3}^{+\bullet}$ and $\mathbf{3}^{2+}$ were obtained using either $CH_2Cl_2$, $(CH_3)_2CO$ or mixtures of the aforementioned solvents and $CH_3CN$. The current–voltage profiles of the CVs are in accordance with previously reported electrochemical data for related TTF-based monolayers, displaying larger peak currents for the formation of the $\mathbf{3}^{2+}$ species compared to those observed for the $\mathbf{3}^{+\bullet}$ state.[9b] The CVs of the SAMs displayed a linear increase in current with scan rate which is indicative of surface-confined behaviour (Fig. 7). The SAMs proved to be remarkably stable, displaying

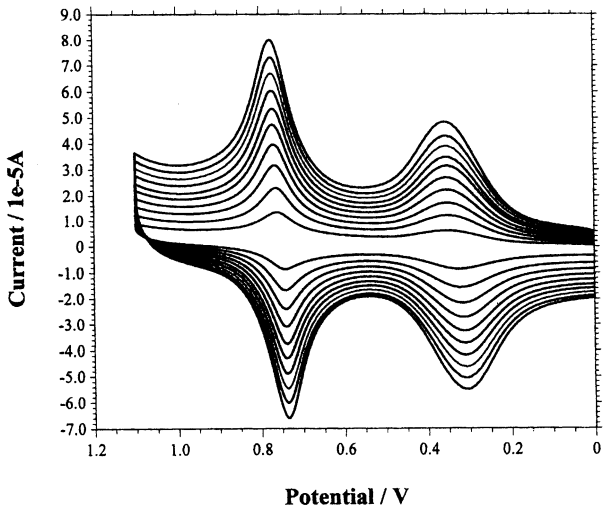


**Fig. 7** Cyclic voltammetry studies of SAMs of **3** recorded at different scan rates: 0.1 (smallest current), 0.2, 0.3, 0.4, 0.5, 0.6, 0.7, 0.8, 0.9, 1.0 V $s^{-1}$ (largest current) [0.1 M $Bu_4NPF_6$ in $CH_2Cl_2$].

the same current response for more than 50 potential scan cycles. Indeed, the SAMs retained their stability over the course of several days.

### Characterization of monolayers by reflection absorption infrared (RAIR) spectroscopy

To further support the proposed self-assembly of **3** (and **1·3**) onto a gold substrate, we have investigated the RAIR spectra of their resulting SAMs. In order to provide a suitable comparison for the RAIR study, we recorded the conventional transmission IR spectra of **1**, **3** and **1·3** (Table 2). Compound **1** displayed major peaks at 1634, 1558, 1504, 1447 1350, 1275, 1226 and 1153 $cm^{-1}$. The strong peak observed at 1634 $cm^{-1}$ is presumably due to the viologen moiety of **1**.[15] Compound **3** displayed strong peaks at 1735, 1615, 1435, 1381, 1229 and 1152 $cm^{-1}$. The peaks at 1735 and 1152 $cm^{-1}$ are characteristic of the –C=O stretch and the symmetric –C–O–C stretch of the ester link unit, respectively.[9b] The IR spectrum of **1·3** gave rise to strong peaks at 1731, 1636 (intense), 1557, 1504, 1447 and 1160 $cm^{-1}$. It is noteworthy that pseudorotaxane formation between **1** and **3** had a slight influence on the vibrational frequency of the –C=O or –C–O–C stretches of **3** (−4 and +8 $cm^{-1}$ difference, respectively).

Fig. 8 shows the absorbance RAIR spectra of monolayers of **3** (Fig. 8a) and **1·3** (Fig. 8b) between 2000 and 1000 $cm^{-1}$. The RAIR spectrum for immobilised **3** is fairly similar to the transmission spectrum of the thin film of **3**. For example, the –C=O stretch and –C–O–C stretches of the ester unit of the self-assembled **3** were clearly visible at 1740 and 1175 $cm^{-1}$, respectively. However, both peaks are shifted to a higher

**Table 2** Summary of the wavenumbers of the major peaks (between 2000 and 1000 $cm^{-1}$) observed by transmission IR spectroscopy of thin films and RAIR spectroscopy of monolayers deposited onto a gold surface

| Transmission IR of **1** | Transmission IR of **3** | Transmission IR of **1·3** | RAIR of **3** | RAIR of **1·3** |
|---|---|---|---|---|
| 1634 | 1735 | 1731 | 1740 | 1726 |
| 1558 | 1615 | 1636 | 1678 | 1637 |
| 1504 | 1435 | 1557 | 1612 | 1555 |
| 1447 | 1381 | 1504 | 1529 | 1502 |
| 1350 | 1229 | 1447 | 1413 | 1447 |
| 1275 | 1152 | 1295 | 1352 | 1429 |
| 1226 | 1087 | 1222 | 1319 | 1381 |
| 1153 | | 1160 | 1175 | 1155 |

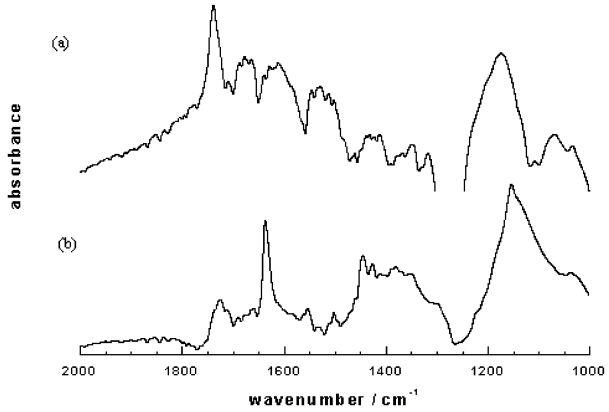


**Fig. 8** RAIR spectra of the monolayers of (a) **3** and (b) **1·3**.

wavenumber, which is in accordance with previously reported data for related systems.[9d] The RAIR spectrum of the self-assembled pseudorotaxane **1·3** clearly displays the –C=O and –C–O–C stretches of the ester unit at 1726 and 1155 $cm^{-1}$, respectively, together with an intense stretch at 1637 $cm^{-1}$. It is noteworthy that the –C=O and –C–O–C stretches of the ester unit of the immobilized pseudorotaxane are shifted to a lower wavenumber compared to the same stretches observed in solution.

### Electrochemically controlled host–guest complexation at the solid/liquid interface

Mixed monolayers were fabricated by immersing a gold wire in an equimolar mixture of **3** (1 mmol) and butyl disulfide (1 mmol) in MeCN for 12 hours.[16] The butyl disulfide was co-assembled with **3** in order to help electronically isolate the TTF units within the SAM, and thus help prevent intermolecular electron transfer reactions taking place. Furthermore, the introduction of the short butyl chains into the SAM architecture should allow the TTF recognition unit to protrude from the surface of the monolayer, thereby facilitating complexation with **1** and **2**. Again, when the CV data were recorded at different scan rates a linear increase in peak currents was observed for the redox waves of the TTF units, which is consistent with the TTF units being surface confined. However, the dilution of the redox-active units of the monolayer resulting from the co-self-assembly with butyl disulfide, had a detrimental effect on the resolution of the redox waves, particularly when scan rates of less than 0.5 V $s^{-1}$ were used. The CVs following the addition of an excess of **1** to the CV cell [0.1 M $Bu_4NPF_6$ in $(CH_3)_2CO$] mirrored the solution-phase studies, as the first oxidation process was immediately shifted by +30 mV, whilst the second oxidation process remained largely unaffected (Fig. 9).[4d] This result shows that one-electron oxidation causes reversible dethreading of the complex, and successive one-electron reduction causes a re-formation. Interestingly, this shift in $E^{1}_{1/2}$ is typically half that observed in solution, presumably due to steric crowding and/or Coulombic repulsion caused by the adjacent pseudorotaxane moieties of the SAM. We have also investigated the electrochemistry of SAMs of **3** [$Bu_4NPF_6$ in $CH_3CN$–$CH_2Cl_2$, (80 : 20, v/v)] in the presence of compound **5**. Similar negative shifts in the half-wave potentials for the $\mathbf{3}^{+\bullet}$ and $\mathbf{3}^{2+}$ states to those obtained for the solution-based experiments were observed (Fig. 10). Moreover, when the experiments were repeated using macrocycle **1** dissolved in $CH_3CN$–$CH_2Cl_2$ (80 : 20, v/v), a +25 mV shift in the redox wave for the $\mathbf{3}^{+\bullet}$ state was observed.

When an excess of **2** was added to the CV cell (0.1 M $Bu_4NPF_6$ in $CH_2Cl_2$) containing a new gold working electrode upon which **3** and butyl disulfide had previously been co-self-assembled, a −25 mV shift of the peak due to the formation of

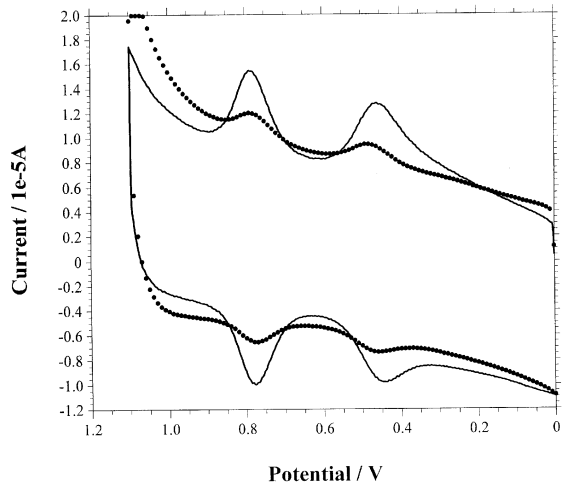


**Fig. 9** Cyclic voltammetry studies of mixed SAMs of **3** (—) and in the presence of an excess of **1** (···) [0.1 M $Bu_4NPF_6$ in $(CH_3)_2CO$].

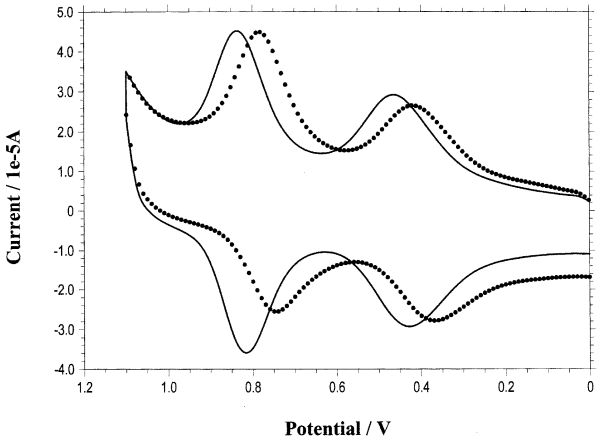


**Fig. 10** Cyclic voltammetry studies of mixed SAMs of **3** (—) and in the presence of an excess of **5** (···) [0.1 M $Bu_4NPF_6$ in $CH_3CN$–$CH_2Cl_2$ (80 : 20, v/v), scan rate = 0.5 V $s^{-1}$].

the $\mathbf{3}^{2+}$ species was observed, corresponding to the immobilized complex undergoing decomplexation when the $\mathbf{3}^{2+}$ is reduced (Fig. 11). Similarly, the observed shift is considerably less than that observed when the electrochemical measurements were performed in solution. It is noteworthy that a small change ($\pm$5 mV) was gradually observed for the redox waves

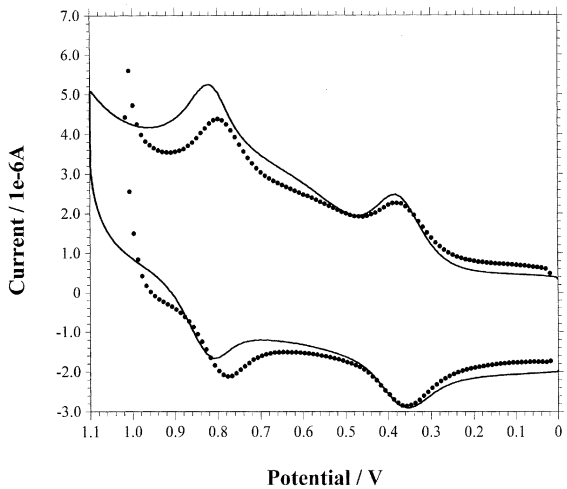


**Fig. 11** Cyclic voltammetry studies of mixed SAMs of **3** (—) and in the presence of an excess of **2** (···) [0.1 M $Bu_4NPF_6$ in $CH_2Cl_2$].

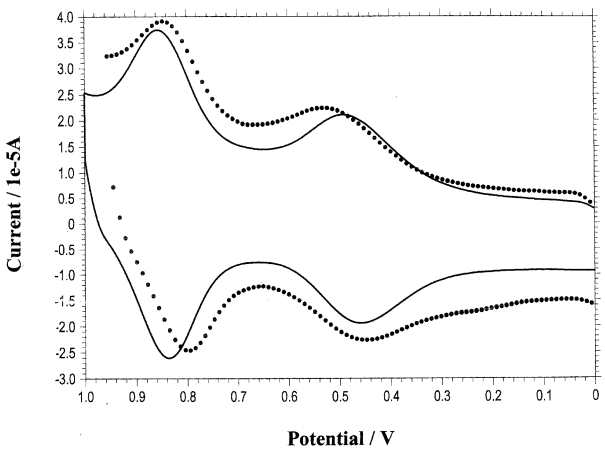


**Fig. 12** CV studies of mixed SAMs of **3** (—) and in the presence of an excess of **1** and **2** (···) [0.1 M $Bu_4NPF_6$ in $CH_3CN$–$CH_2Cl_2$ (80 : 20, v/v)].

corresponding to the formation of the $\mathbf{3}^{+\bullet}$ state when **2** was added, or alternatively to the $\mathbf{3}^{2+}$ state when **1** was added to the CV cell following repeated redox cycling.

With electrochemically controlled complexation of immobilized **3** with separate solutions of macrocycles **1** and **2** confirmed, we next investigated these processes using SAMs of **3** in the presence of both **1** and **2**. Excess **1** and **2** were added to a CV cell containing a new gold working electrode upon which **3** and butyl disulfide had previously been co-self-assembled, and the CVs were recorded [0.1 M $Bu_4NPF_6$ in $CH_3CN$–$CH_2Cl_2$, 80 : 20]. In most instances a decrease in the reversibility of the redox wave of the $\mathbf{3}^{2+}$ state was observed upon increasing the scan rate. Unfortunately, data at low scan rates were not readily obtainable, as experiments performed at scan rates below 0.1 V $s^{-1}$ failed to provide meaningful data as the redox waves of the immobilised TTF units became rather poorly resolved. However, at a scan rate of 0.1 V $s^{-1}$, reasonably reversible and well defined waveforms were usually obtained, which indicated that a +20 mV shift in the half-wave potential for the $\mathbf{3}^{+\bullet}$ state and a −20 mV shift in the half-wave potential for $\mathbf{3}^{2+}$ occurred upon the addition of both macrocycles to the electrolyte solution (Fig. 12). The shifts correspond fairly well to those obtained for **3** in solution upon the addition of **1** and **2**, and indicate that the immobilized TTF guest interchanges between the two macrocyclic host units upon altering its oxidation state from 0 to 2+.[4d] However, it must be stressed that the redox waves for the TTF unit became poorly defined following repeated electrochemical cycling, and in some instances, the shift in the half-wave potential that signals electrochemically controlled host–guest complexation totally disappeared after two or three redox cycles.

## 4. Conclusions

In summary, we have shown that we can exploit the multi-stage redox properties of SAMs of **3** to produce surfaces with electrochemically controllable binding properties. Depending on the oxidation state of the immobilized guest unit, the TTF moiety can either form a pseudorotaxane with **1** in its neutral state, or form a pseudorotaxane with **2** in its dicationic state. However, the reversibility of the electrochemically controlled surface confined pseudorotaxane architectures formed by sequentially oxidising the TTF moiety of the SAMs in the presence of both macrocycles was poor, which will significantly hamper the fabrication of usable devices from these systems. If improvements in this reversibility can be achieved, the ability to control the selective binding between the immobilized guest and disparate host species using this electrochemical Umpolung, offers an exciting opportunity to reversibly and

combinatorially tailor surface properties and function. Work is underway in our laboratories to develop new surface confined multi-pole switches based upon pseudorotaxanes with more reversible redox controlled architectures. Furthermore, we are currently developing electrochemically controllable surface confined rotaxane-based systems, where the more environmentally robust nature of these supramolecules should lead to development of useable components for the emerging molecular electronics industries. The results of these studies will be reported in due course.

## 5. Experimental section

### General

Melting points are uncorrected. $^1$H NMR chemical shifts, given in ppm, are relative to tetramethylsilane as internal standard and were recorded on a Bruker AC 200 spectrometer. $^{13}$C NMR chemical shifts, given in ppm, are relative to tetramethylsilane as internal standard and were recorded on a Bruker DPX 400 spectrometer. EI mass spectra were recorded on a Finnigan MAT 900 XLT spectrometer and FAB-MS were recorded on a Micromass Autospec instrument. Solution UV-vis spectra were recorded on a Shimadzu UV-160A spectrometer in quartz cells.

### Synthesis of 3

To a stirred solution 4-hydroxymethyl-trimethyl-TTF[13] (0.1 g, 0.36 mmol) and thioctic acid (0.074 g, 0.36 mmol) in dry THF (100 mL) was added DCC (0.074 g, 0.36 mmol) and DMAP (0.044 g, 0.36 mmol). The resulting solution was stirred under a nitrogen atmosphere for 24 h at 25 °C. The solvent was removed under reduced pressure, and the crude product was purified using column chromatography (neutral alumina, toluene). Compound **3** was isolated as a salmon pink solid (0.13 g, 77%). Mp 88–90 °C. $^1$H NMR [$CO(CD_3)_2$–TMS]: 4.85 (s, 2 H), 3.62 (m, 1 H), 3.16 (m, 2 H), 2.48 (m, 1 H), 2.38 (t, 2 H), 2.10 (s, 3 H), 1.96 (s, 6 H), 1.90 (m, 1 H), 1.65 (m, 4 H) 1.50 (m, 2 H); $^{13}$C NMR ($CO(CD_3)_2$–TMS): 173.15, 131.23, 124.43, 123.78, 123.72 109.11, 106.33, 58.67, 57.13, 40.88, 39.08, 35.29, 34.17, 25.41, 13.90, 13.60, 13.58; MS (EI) $m/z$ = 464 ($M^+$). Calc. for $C_{18}H_{24}O_2S_6$: C, 46.55; H, 5.17. Found: C, 46.58; H, 5.20%.

### Synthesis of 1·3

To a stirred solution of **3** (0.02 g, 0.04 mmol) in $CH_3CN$ (10 mL) was added **1** (0.044 g, 0.04 mmol). The resulting emerald green solution was stirred for 0.5 h, and the solvent was allowed to slowly evaporate to approximately one quarter of its original volume over the course of 2 days. The resulting green powder was removed by filtration, and dried under high vacuum for 2 h. Mp 189 °C (dec.). $^1$H NMR ($CO(CD_3)_2$–TMS) 9.53 (d, 8 H), 8.42 (d, 8 H), 8.01 (s, 8 H), 6.07 (s, 8 H), 4.92 (s, 2 H), 3.63 (m, 1 H), 3.15 (m, 2 H), 2.63 (t, 2 H), 2.48 (m, 1 H), 2.19 (s, 3 H), 1.92 (m, 1 H), 1.82 (s, 6 H), 1.60 (m, 4 H), 1.35 (m, 2 H); MS (FAB) $m/z$ = 1565 ($M^+$). Calc. for $C_{54}H_{56}N_4F_{24}O_2P_4S_6$: C, 41.41; H, 3.58; N, 3.58. Found: C, 41.50; H, 3.60; N, 3.65%.

### Molecular modelling studies

Calculations were performed using HyperChem 5.11. Geometries of **1** and **3** were optimised at the AM1 level of theory. The resulting structures were merged, and the geometry of the resulting complex was re-optimised using the MM+ forcefield.[10]

### Electrochemical measurements

All electrochemical experiments were performed using a CH Instruments CH120A electrochemical workstation. Electrolyte solutions were prepared from recrystallized $Bu_4NPF_6$ using spectroscopic grade $(CH_3)_2CO$, $CH_3CN$ or $CH_2Cl_2$ and purged with nitrogen prior to use. A three electrode configuration was used with a Ag/AgCl reference electrode and a platinum wire as the counter electrode. For the solution studies a platinum disc working electrode was used. The SAM studies used a gold wire (70 × 0.5 mm) working electrode (see below), upon which butyl disulfide and/or compound **3** had been previously self-assembled. The scan rate for the experiments, unless otherwise stated, was 0.1 V s$^{-1}$.

### Monolayer preparation

The gold (99.999%) electrodes were prepared from a 70 mm long gold wire (diameter = 0.5 mm). The wire electrodes were cleaned using previously reported procedures.[17] In order to facilitate the detection of host–guest complexation at surfaces, electrodes with large surface areas were fabricated by coiling the wires around a 2 mm diameter rod prior to the self-assembly of **3**. This ensured that reasonable peak currents for the redox waves of the TTF units were observed at reasonably slow scan rates. The SAM modified electrodes were prepared by immersing the gold wires in a solution of **3** (1 mmol) or butyl disulfide and **3** (1 mmol of each component) in acetonitrile for 24 h. After removal from solution, the electrodes were rinsed with copious amounts of THF and $CH_3CN$ and dried in air.

### Infrared spectroscopy

Transmission IR spectra were recorded as thin films using a Perkin-Elmer RX FT-IR system (4 scans with 4 cm$^{-1}$ resolution). Samples of **1**, **3** and **1·3** were dissolved in spectroscopic grade $CH_3CN$ and a drop of this solution was transferred to a NaCl disc. The solvent was allowed to evaporate overnight, and the discs were then dried under high-vacuum for 2 h. The reflection absorption IR spectra (RAIRs) were recorded on a Bruker IFS 66 v/S spectrometer equipped with a variable angle infra-red reflection accessory set at 80°. The spectra were measured using a liquid nitrogen cooled MCT detector. The measurement chamber was evacuated ($P$ = 0.004 mbar) during the measurements. 500 Scans with 4 cm$^{-1}$ resolution were performed to obtain the spectra. The gold substrates consisted of 200 nm of vapour-deposited Au on top of glass microscope slides. Monolayers of **3** and **1·3** were prepared by immersing the gold slide in a $10^{-5}$ M solution of the disulfide for 24 h. When the gold slides were removed from solution, they were thoroughly rinsed with MeCN and then THF and dried under high-vacuum for 1 h.

## Acknowledgements

G. C. gratefully acknowledges the EPSRC and The Royal Society for supporting this work. D. F. P. thanks the EPSRC for financial support. V. M. R. acknowledges the NSF for grant CHE-9905492. We thank the EPSRC Mass Spectrometry Service Centre, Swansea, for obtaining EI- and FAB-MS data.

## References

1 For recent reviews of supramolecular electrochemistry, see: (*a*) A. E. Kaifer and M. Gómez-Kaifer, *Supramolecular Electrochemistry*, Wiley-VCH, Weinheim, 1999; (*b*) P. L. Boulas, M. Gomez-Kaifer and L. Echegoyen, *Angew. Chem., Int. Ed.*, 1998, **37**, 216; (*c*) V. M. Rotello and A. Niemz, *Acc. Chem. Res.*, 1999, **32**, 44; (*d*) A. E. Kaifer, *Acc. Chem. Res.*, 1999, **32**, 62; (*e*) J. H. R. Tucker and S. Collinson, *Chem. Soc. Rev.*, 2002, **31**, 147.

2 A. Mirzoian and A. E. Kaifer, *Chem. Eur. J.*, 1997, **3**, 1052.

3 For recent examples, see: (*a*) J. D. Carr, L. Lambert, D. E. Hibbs, M. B. Hursthouse, K. M. A. Malik and J. H. R. Tucker, *Chem. Commun.*, 1997, 649; (*b*) J. D. Carr, S. J. Coles, M. B. Hursthouse, M. E. Light, J. H. R. Tucker and J. Westwood, *Angew. Chem., Int. Ed.*, 2000, **39**, 3296; (*c*) S. R. Collinson, T. Gelbrich, M. B. Hursthouse and J. H. R. Tucker, *Chem. Commun.*, 2001, 555; (*d*) Y. Ge, R. R. Lilienthal and D. K. Smith, *J. Am. Chem. Soc.*, 1996, **118**, 3976; (*e*) Y. Ge, L. Miller, T. Ouimet and D. K. Smith, *J. Org. Chem.*, 2000, **65**, 8831; (*f*) E. Breinlinger, A. Niemz and V. M. Rotello, *J. Am. Chem. Soc.*, 1995, **117**, 5379; (*g*) C. Bourgel, A. S. F. Boyd, G. Cooke, H. A. de Cremiers, F. M. A. Duclairoir and V. M. Rotello, *Chem. Commun.*, 2001, 1954.

4 For recent examples, see: (*a*) W. Devonport, M. A. Blower, M. R. Bryce and L. M. Goldenberg, *J. Org. Chem.*, 1997, **62**, 885; (*b*) P. L. Anelli, M. Asakawa, P. R. Ashton, R. A. Bissell, G. Clavier, R. Górski, A. E. Kaifer, S. J. Langford, G. Mattersteig, S. Menzer, D. Philp, A. M. Z. Slawin, N. Spencer, J. F. Stoddart, M. S. Tolley and D. J. Williams, *Chem. Eur. J.*, 1997, **3**, 1113; (*c*) M. Asakawa, P. R. Ashton, V. Balzani, A. Credi, G. Mattersteig, O. A. Matthews, M. Montalti, N. Spencer, J. F. Stoddart and M. Venturi, *Chem. Eur. J.*, 1997, **3**, 1992; (*d*) P. R. Ashton, V. Balzani, J. Becher, A. Credi, M. C. T. Fyfe, G. Mattersteig, S. Menzer, M. B. Nielsen, F. M. Raymo, J. F. Stoddart, M. Venturi and D. J. Williams, *J. Am. Chem. Soc.*, 1999, **121**, 3951; (*e*) V. Balzani, J. Becher, A. Credi, M. B. Nielsen, F. M. Raymo, J. F. Stoddart, A. M. Talarico and M. Venturi, *J. Org. Chem.*, 2000, **65**, 1947.

5 For recent examples of redox active monolayers with chemically controllable structures, see: (*a*) M. Asakawa, M. Higuchi, G. Mattersteig, T. Nakamura, A. R. Pease, F. M. Raymo, T. Schimizu and J. F. Stoddart, *Adv. Mater.*, 2000, **12**, 1099; (*b*) S. Chia, J. Cao, J. F. Stoddart and J. I. Zink, *Angew. Chem., Int. Ed.*, 2001, **40**, 2447.

6 For recent examples or redox active monolayers with electrochemically controllable recognition properties, see: (*a*) A. K. Boal and V. M. Rotello, *J. Am. Chem. Soc.*, 1999, **121**, 4915; (*b*) C. P. Collier, E. W. Wong, M. Belohradsky, F. M. Raymo, J. F. Stoddart, P. J. Keukes, R. S. Williams and J. R. Heath, *Science*, 1999, **285**, 391; (*c*) A. K. Boal and V. M. Rotello, *J. Am. Chem. Soc.*, 2000, **122**, 734; (*d*) G. Cooke, F. M. A. Duclairoir, V. M. Rotello and J. F. Stoddart, *Tetrahedron. Lett.*, 2000, **41**, 8163; (*e*) C. P. Collier, G. Mattersteig, E. W. Wong, Y. Luo, K. Beverly, J. Sampaio, F. M. Raymo, J. F. Stoddart and J. R. Heath, *Science*, 2000, **289**, 1172; (*f*) Y. Ge and D. K. Smith, *Anal. Chem.*, 2000, **72**, 1860; (*g*) A. Labande and D. Astruc, *Chem. Commun.*, 2000, 1007; (*h*) M.-C. Daniel, J. Ruiz, S. Nlate, J. Palumbo, J.-C. Blais and D. Astruc, *Chem. Commun.*, 2001, 2000; (*i*) C. P. Collier, J. O. Jeppersen, Y. Luo, J. Perkins, E. W. Wong, J. R. Heath and J. F. Stoddart, *J. Am. Chem. Soc.*, 2001, **123**, 12632; (*j*) A. K. Boal and V. M. Rotello, *J. Am. Chem. Soc.*, 2002, **124**, 5019; (*k*) H. M. Goldston, A. N. Scribner, S. A. Trammell and L. M. Tender, *Chem. Commun.*, 2002, 416; (*l*) Y. Luo, C. P. Collier, J. O. Jeppesen, K. A. Nielsen, E. Delonno, G. Ho, J. Perkins, H.-R. Tseng, T. Yamamoto, J. F. Stoddart and J. R. Heath, *Chem. Phys. Chem.*, 2002, **3**, 519.

7 (*a*) A. R. Pease, J. O. Jeppesen, J. F. Stoddart, Y. Luo, C. P. Collier and J. R. Heath, *Acc. Chem. Res.*, 2001, **34**, 433; (*b*) A. R. Pease and J. F. Stoddart, *Struct. Bonding (Berlin)*, 2001, **99**, 189; (*c*) F. Raymo and J. F. Stoddart, *Molecular Switches*, Ed. B. L. Feringa, Wiley-VCH, Weinheim, 2001, p. 219; (*d*) V. Balzani, M. Venturi and A. Credi, *Molecular Devices and Machines-A Journey into the Nanoworld*, Wiley-VCH, Weinheim, 2003.

8 D. Philp, A. M. Z. Slawin, N. Spencer, J. F. Stoddart and D. J. Williams, *J. Chem. Soc., Chem. Commun.*, 1991, 1584.

9 For recent examples of TTF-based SAMs deposited on gold electrodes, see: (*a*) A. J. Moore, L. M. Goldenberg, M. R. Bryce, M. C. Petty, A. P. Monkman, C. Marenco, J. Yarwood, M. J. Joyce and S. N. Port, *Adv. Mater.*, 1998, **10**, 395; (*b*) H. Fujihara, H. Nakai, M. Yoshihara and T. Maeshima, *Chem. Commun.*, 1999, 737; (*c*) H. Liu, S. Liu and L. Echegoyen, *Chem. Commun.*, 1999, 1493; (*d*) S.-G. Liu, H. Liu, K. Bandyopadhyay, Z. Gao and L. Echegoyen, *J. Org. Chem.*, 2000, **65**, 3292; (*e*) M. Fibbioli, K. Bandyopadhyay, S.-G. Liu, L. Echegoyen, O. Enger, F. Diederich, P. Bühlmann and E. Pretsch, *Chem. Commun.*, 2000, 339; (*f*) A. J. Moore, L. M. Goldenberg, M. R. Bryce, M. C. Petty, J. Moloney, J. A. K. Howard, M. J. Joyce and S. N. Port, *J. Org. Chem.*, 2000, **65**, 8269.

10 M. R. Bryce, G. Cooke, F. M. A. Duclairoir and V. M. Rotello, *Tetrahedron Lett.*, 2001, **42**, 1143.

11 B. Odell, M. V. Reddington, A. M. Z. Slawin, N. Spencer, J. F. Stoddart and D. J. Williams, *Angew. Chem., Int. Ed.*, 1988, **27**, 1547.

12 P. R. Ashton, E. J. T. Chrystal, J. P. Mathias, K. P. Parry, A. M. Z. Slawin, N. Spencer, J. F. Stoddart and D. J. Williams, *Tetrahedron Lett.*, 1987, **28**, 6367.

13 A. J. Moore, M. R. Bryce, A. S. Batsanov, J. C. Cole and J. A. K. Howard, *Synthesis*, 1995, 675.

14 H. M. Colquhoun, E. P. Gooding, J. M. Maud, J. F. Stoddart, J. B. Wolstenholme and D. J. Williams, *J. Chem. Soc., Perkin Trans. 2*, 1985, 607.

15 R. E. Hester and S. Suzuki, *J. Phys. Chem.*, 1982, **86**, 4626.

16 Mixed monolayers were also fabricated onto gold bead electrodes (formed using previously reported procedures), which are known to afford well-defined Au(111) facets.[9d] Although the appearance of the resulting waves was in accordance with the CV's obtained using the gold wire electrodes, the resolution of the $\mathbf{3}^{+\bullet}$ and $\mathbf{3}^{2+}$ redox waves for the SAM modified gold bead electrodes were poor in comparison with the gold wire electrodes. Therefore, as shifts in the $\mathbf{3}^{+\bullet}$ and $\mathbf{3}^{2+}$ waves are crucial for proving the electrochemically controlled complexation–decomplexation with **1** or **2**, for this study we have opted for gold wire rather than gold bead working electrodes.

17 S. E. Creager, L. A. Hockett and G. K. Rowe, *Langmuir*, 1992, **8**, 854.